

# Studying the Perturbative Reggeon

S. Griffiths

and

D.A. Ross

Physics Department,  
University of Southampton,  
Southampton SO17 1BJ, United Kingdom

## ABSTRACT

We consider the flavour non-singlet Reggeon within the context of perturbative QCD. This consists of ladders built out of “reggeized” quarks. We propose a method for the numerical solution of the integro-differential equation for the amplitude describing the exchange of such a Reggeon. The solution is known to have a sharp rise at low values of Bjorken- $x$  when applied to non-singlet quantities in deep-inelastic scattering. We show that when the running of the coupling is taken into account this sharp rise is further enhanced, although the  $Q^2$  dependence is suppressed by the introduction of the running coupling. We also investigate the effects of simulating non-perturbative physics by introducing a constituent mass for the soft quarks and an effective mass for the soft gluons exchanged in the  $t$ -channel.

# 1 Introduction

In recent years, much attention has been given to the perturbative QCD simulation of the Pomeron. The reason for this is that the reach of HERA is such that one now has data on structure functions and differential cross-sections for other inclusive processes which are well into the diffractive region (low- $x$ ) whilst at the same time maintaining momentum scales for *all* the kinematic variables. These variables are large enough that a renormalization-group improved perturbative expansion summed to all orders in leading  $\ln x$  is expected to be valid. This is the region in which one expects to be able to test the BFKL Pomeron [1]. Notwithstanding this, it should be recalled that the original motivation for the study of the Pomeron in QCD was an attempt to explain how the successes of Regge theory could be under-written by a quantum field theory.

Somewhat less emphasis has been placed on the Regge trajectory below the Pomeron (the Reggeon) for which phenomenological fits [2] have shown have an intercept  $\approx \frac{1}{2}$ . In the same way that the QCD Pomeron is constructed from ladders of reggeized gluons with a colour singlet projection, so the QCD Reggeon is constructed from ladders of a reggeized quark-antiquark pair, again with colour singlet projection.

The cleanest way to distinguish between Pomeron dominated processes and Reggeon dominated processes is to note that a quark-antiquark pair can be in a flavour non-singlet state. We therefore consider quantities which are controlled by flavour non-singlet operators. Such quantities include the structure function  $F_3$  in deep-inelastic scattering, or the spin-dependent structure functions. The Reggeon is only expected to dominate such quantities at sufficiently low- $x$ , and the extraction of low- $x$  data for such quantities is very difficult. The spin-dependent structure functions at low- $x$  have recently been considered in ref.[3]. At the moment the lowest values of  $x$  for which we have data on  $F_3$  are not yet in the asymptotic region where we would expect the Reggeon to dominate, but on the other hand they are not very far away and in the same way that HERA is currently used to test the QCD Pomeron, the QCD Reggeon could reasonably be expected to be probed in the not-too-distant future.

In order to construct the Reggeon within the context of perturbative QCD, one needs first to establish that the quark reggeizes, in the same way that the gluon reggeizes. In other words, it is necessary to show that to leading order in  $\ln s$ , the amplitude in which the quantum numbers of a quark is exchanged in the  $t$ -channel, has an  $s$  dependence given by

$$s^{\alpha_{\mathcal{Q}}(t)}.$$

From standard partial wave analysis we expect  $\alpha_{\mathcal{Q}}(t) = \frac{1}{2}$  in leading order and for the  $t$  dependence to arise from higher order corrections. This was first established some time ago [4]. However, we feel that several important features of this derivation were not sufficiently clearly explained in ref.[4]. We have repeated the relevant calculations and we briefly review our method for deriving the reggeization of the quark in section 2. Once quark reggeization has been established, an integro-differential equation can be established for the sum of the leading  $\ln s$  parts of the amplitude for the exchange of the quantum numbers of the Reggeon. This has been derived in ref.[5] and we quote the result in section 3. This equation can, in principle, be solved analytically since it involves a kernel which is conformally invariant (in

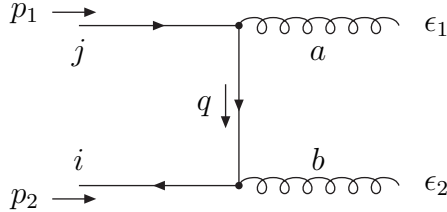


Figure 2.1: The tree-level exchange of a soft quark

two dimensions) such that its eigenfunctions are the representations of the conformal group. Unlike the case of the Pomeron the leading eigenvalue is *not* analytic in the coupling. This causes severe difficulties when one tries to reproduce the analytic results by numerical means. We propose a programme for numerical solution of the integro-differential equation which is consistent with the known asymptotic behaviour. This allows one to introduce modifications to the kernel, such as the running of the coupling, which breaks conformal invariance, so that the analytic approach is no longer viable, but the numerical approach remains reliable.

In section 4 we apply this to a model of flavour non-singlet deep-inelastic scattering. We call this a model since an arbitrary function has to be taken for the impact factor describing the emission of a Reggeon from the target hadron. However, we do not expect either the  $x$  dependence at sufficiently low  $x$ , or the  $Q^2$  at sufficiently high  $Q^2$  to be particularly sensitive to the exact nature of this impact factor. We look at the effect of running the coupling and observe that whereas this further enhances the predicted rise in the non-singlet structure functions as  $x \rightarrow 0$ , it suppresses the  $Q^2$  dependence of such structure functions. Finally, we postulate that the most significant feature of non-perturbative effects in the case of the Reggeon is to provide the soft quark and antiquark exchanged in the  $t$ -channel with a constituent mass, and the soft gluons an effective mass. We therefore solve the modified equation for the Reggeon in which a mass is assigned to the soft particles. We find that this significantly suppresses the low- $x$  rise and that this suppression extends to values of  $Q^2$  way beyond the assigned values of the constituent mass. In section 5 we summarize our conclusions.

## 2 The Reggeized Quark

In this section we review the derivation of the “reggeized quark”. The result obtained agrees with that previously obtained [4], but in our derivation some of the subtleties leading to the result are discussed in more detail.

We begin by considering the process

$$q + \bar{q} \rightarrow g + g, \quad (2.1)$$

in the Regge regime,  $s \gg |t|$ , where a soft quark is exchanged in the  $t$ -channel as shown in

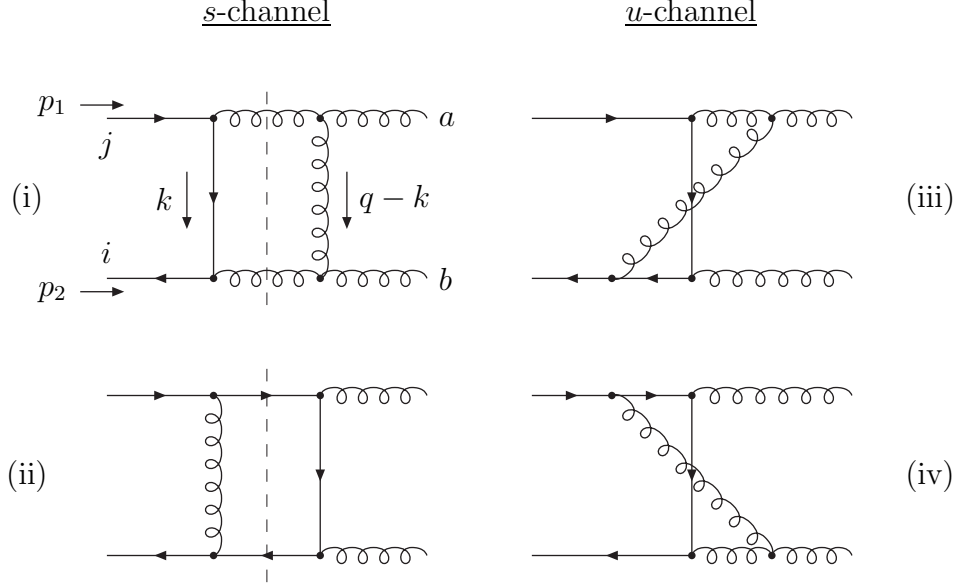


Figure 2.2: One-loop leading  $\ln s$  corrections to  $q + \bar{q} \rightarrow g + g$ . The 2-body cuts in the  $s$ -channel are shown, however (iii) and (iv) have similar cuts in the  $u$ -channel

Fig. 2.1. The amplitude is given by

$$\mathcal{A}_0(q) = (\tau^b \tau^a)_{ij} 2\pi\alpha_s \bar{v}(p_2) \gamma u(p_1) \frac{\epsilon_2^* q \epsilon_1^*}{|q|^2} + \text{h.c.}, \quad (2.2)$$

where we have introduced holomorphic coordinates in the plane transverse to the incident momenta  $p_1$  and  $p_2$  such that  $\gamma$  ( $\gamma^*$ ) are the  $\gamma$ -matrices in this plane,  $q$  ( $q^*$ ) are the components of the transverse momentum transferred in the  $t$ -channel, and  $\epsilon_1$  ( $\epsilon_1^*$ ) and  $\epsilon_2$  ( $\epsilon_2^*$ ) are the polarisation vectors of the outgoing gluons.

We now consider the one-loop corrections which are proportional to  $\ln s$ , since it is only these contributions that are relevant for reggeization. The relevant diagrams are shown in Fig. 2.2, and each of these gives the same contribution (up to a colour factor), which may be written as <sup>1</sup>

$$\frac{\alpha_s^2}{\pi} \ln \left( \frac{s}{\mathbf{k}^2} \right) \bar{v}(p_2) \gamma u(p_1) \epsilon_2^* \epsilon_1^* \int d^2 \mathbf{k} \frac{k}{|k|^2 |q-k|^2} + \text{h.c.} \quad (2.3)$$

The diagrams of Fig. 2.2 have colour factors

---

<sup>1</sup> The quantity  $\mathbf{k}^2$ , used to scale  $s$  inside the logarithms is understood to be a square momentum which is of the order of the square momentum transfer  $|t|$ , or some other momentum ( $\ll s$ ) involved in the coupling of the Reggeon at the top or bottom of the ladder. Since we are confining our discussion to leading logarithm, its exact value is unimportant.

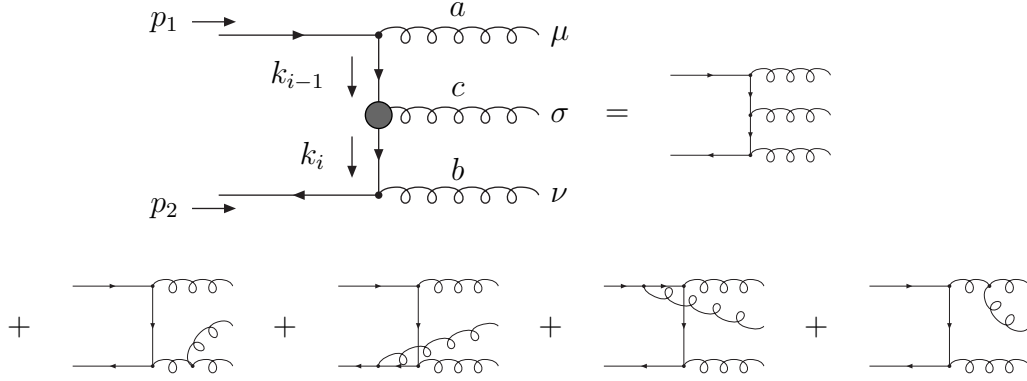


Figure 2.3: The effective quark-gluon vertex

$$\frac{N}{2} (\tau^b \tau^a)_{ij} + \frac{1}{4} \delta^{ab} \delta_{ij} \quad (\text{i})$$

$$\frac{-1}{2N} (\tau^b \tau^a)_{ij} + \frac{1}{4} \delta^{ab} \delta_{ij} \quad (\text{ii})$$

$$-\frac{1}{4} \delta^{ab} \delta_{ij} \quad (\text{iii})$$

$$-\frac{1}{4} \delta^{ab} \delta_{ij} \quad (\text{iv})$$

where  $N (= 3)$  is the number of colours.

Adding these one-loop contributions we obtain the result for the one-loop correction to be

$$\mathcal{A}_1(q) = \mathcal{A}_0(q) \ln \left( \frac{s}{\mathbf{k}^2} \right) \epsilon_{\mathcal{Q}}(q) \quad (2.4)$$

with

$$\epsilon_{\mathcal{Q}}(q) = -C_F \frac{\alpha_s}{2\pi^2} \int d^2 \mathbf{k} \frac{k q^*}{|k|^2 |q - k|^2}, \quad (2.5)$$

and  $C_F = (N^2 - 1)/2N$ .

At the next order a number of complications occur, some of which are common to the problem of gluon reggeization [1]. The first of these is that the diagrams that contribute in leading  $\ln s$  are *not* all of the ladder type. However, all diagrams whose  $s$ -channel cuts contain three intermediate particles can be reduced to a ladder-type diagram using an effective vertex. This is demonstrated in Fig. 2.3. The Feynman rule for this effective vertex involves the substitution of  $\gamma^\sigma$  in the standard rule with  $\Gamma_{\mathcal{Q}}^\sigma$ , where

$$\Gamma_{\mathcal{Q}}^\sigma(k_{i-1}, k_i) = \gamma^\sigma + \frac{2p_1^\sigma k_{i-1}}{\beta_i s} + \frac{2p_2^\sigma k_i}{\alpha_{i-1} s} \quad (2.6)$$

from which it follows that

$$\bar{v}(p_2) (\Gamma_{\mathcal{Q}} \cdot \epsilon_i) u(p_1) = \bar{v}(p_2) \gamma u(p_1) \frac{1}{2} \left( \frac{\epsilon_i k_{i-1}^*}{k_{i-1} - k_i} + \frac{\epsilon_i^* k_i^*}{k_{i-1}^* - k_i^*} \right) + \text{h.c.} \quad (2.7)$$

$k_{i-1}$ ,  $k_i$  are the transverse momenta of the incoming and outgoing quarks, defined in terms of Sudakov variables by

$$k_i^\mu = \alpha_i p_1^\mu + \beta_i p_2^\mu + k_{\perp i}^\mu$$

with  $k_{\perp i}^2 = -|k_i|^2$ .

We also need the equivalent effective vertex for the emission of a gluon with polarisation  $\epsilon_i$  from incoming and outgoing vertical gluon lines with momenta  $k_{i-1}$ ,  $k_i$  and Lorentz indices  $\mu$ ,  $\nu$ . This is given by

$$\Gamma_{\mathcal{G}}^{\mu\nu}(k_i, k_{i-1}) \cdot \epsilon_i = \frac{2p_2^\mu p_1^\nu}{s} \left( \frac{\epsilon_i k_{i-1}^* k_i}{k_i - k_{i-1}} + \text{h.c.} \right). \quad (2.8)$$

In both of these effective vertices, we have assumed the multi-Regge kinematics, namely

$$\alpha_{i-1} \gg \alpha_i$$

$$|\beta_i| \gg |\beta_{i-1}|.$$

The product of these two effective vertices, summed over the polarisations for the emitted gluon is given by

$$\sum_{\text{pol'ns}} (\Gamma_{\mathcal{G}} \cdot \epsilon)(\Gamma_{\mathcal{Q}} \cdot \epsilon) = \gamma \left( q^* - \frac{k'^* |q - k|^2}{|k - k'|^2} - \frac{k^* |q - k'|^2}{|k - k'|^2} \right) + \text{h.c.} \quad (2.9)$$

A further complication arises from the need to consider diagrams in which the central cut line involves a quark or antiquark (as opposed to a gluon) and this is demonstrated pictorially in Fig. 2.4.

Piecing all this together with the appropriate colour factors we find that the contribution from all such diagrams may be written as

$$\mathcal{A}_2(q) = \frac{1}{2} (\epsilon_{\mathcal{Q}}(q))^2 \mathcal{A}_0(q) + \mathcal{A}_2(q)' \quad (2.10)$$

where

$$\begin{aligned} \mathcal{A}_2(q)' = & - \left( C_F + \frac{N}{2} \right) C_F (\tau^b \tau^a)_{ij} \frac{\alpha_s^3}{4\pi^3} \ln^2 \left( \frac{s}{\mathbf{k}^2} \right) \bar{v}(p_2) \gamma u(p_1) \epsilon_2^* \epsilon_1^* \\ & \times \int d^2 \mathbf{k}_1 d^2 \mathbf{k}_2 \frac{1}{|k_2|^2 |q - k_1|^2 |k_1 - k_2|^2} + \text{h.c.} \end{aligned}$$

The first term suggests that the amplitude is indeed “reggeizing”, whereas the contribution  $\mathcal{A}_2(q)'$  cancels against the diagrams shown in Fig. 2.5, in which there are two particles in each ( $s$ -channel or  $u$ -channel) cut and where the loop on either side of this cut is interpreted as the reggeization of the vertical quark or gluon line. We have now developed a general mechanism for the derivation of the reggeized quark, using the traditional “bootstrap” approach. We make the ansatz that the quark reggeizes, with Regge trajectory given by  $1/2 + \epsilon_{\mathcal{Q}}(q)$  as

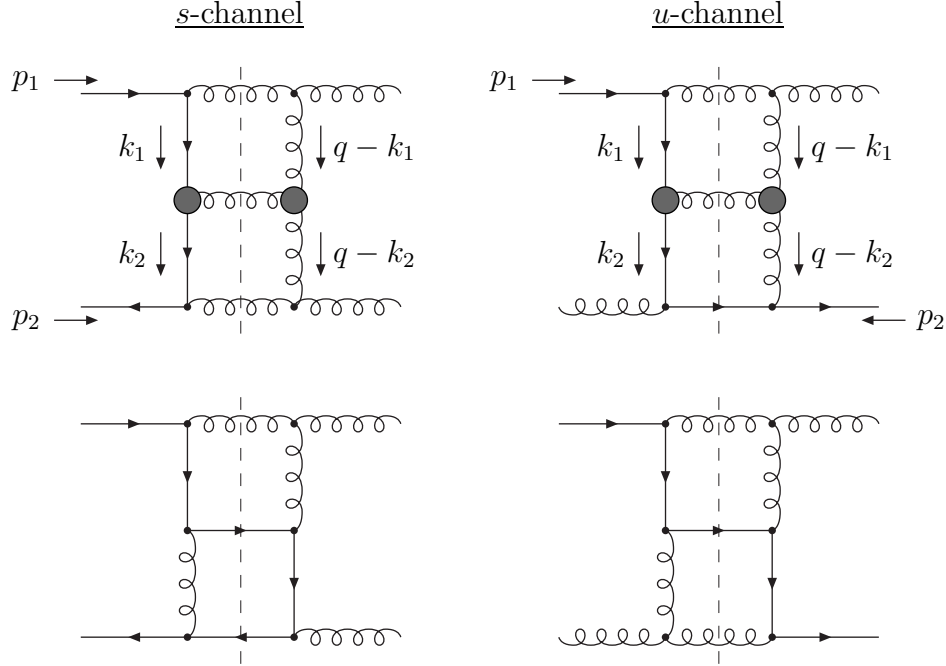


Figure 2.4: Examples of 2-loop ladders. Diagrams with a quark or antiquark rung have to be considered in addition to the gluon rungs with effective vertices

defined in (2.5) and show that this ansatz is self-consistent (the summand of  $1/2$  will be explained shortly). We also need to make use of the reggeization of the gluon which has a Regge trajectory of  $1 + \epsilon_{\mathcal{G}}(q)$  with

$$\epsilon_{\mathcal{G}}(q) = -\frac{N}{2} \frac{\alpha_s}{2\pi^2} \int d^2\mathbf{k} \frac{|q|^2}{|k|^2 |k-q|^2}. \quad (2.11)$$

In order to develop an expression for the amplitude for the process (2.1), whose iterative solution gives a series

$$\mathcal{A}_0(q) + \mathcal{A}_1(q) + \mathcal{A}_2(q) + \dots,$$

we need to consider the addition of both gluon *and* quark or antiquark rungs. This is demonstrated in Fig. 2.6. In general these ladder diagrams lead to an integro-differential equation of the form

$$\frac{\partial F(s, k, q)}{\partial \ln s} = \int d^2\mathbf{k}' \mathcal{K}(k, k', q) F(s, k', q), \quad (2.12)$$

in which the kernel,  $\mathcal{K}$ , may be divided into two parts. The effect of adding a rung gives a contribution of

$$\mathcal{K}^{\text{rung}}(k, k', q) = -\frac{\alpha_s}{2\pi^2} \frac{k'}{|k'|^2 |q-k'|^2} \left( C_F q^* - C_F \frac{k^* |q-k'|^2}{|k-k'|^2} - \frac{N}{2} \frac{k'^* |q-k|^2}{|k-k'|^2} \right) + \text{h.c.} \quad (2.13)$$

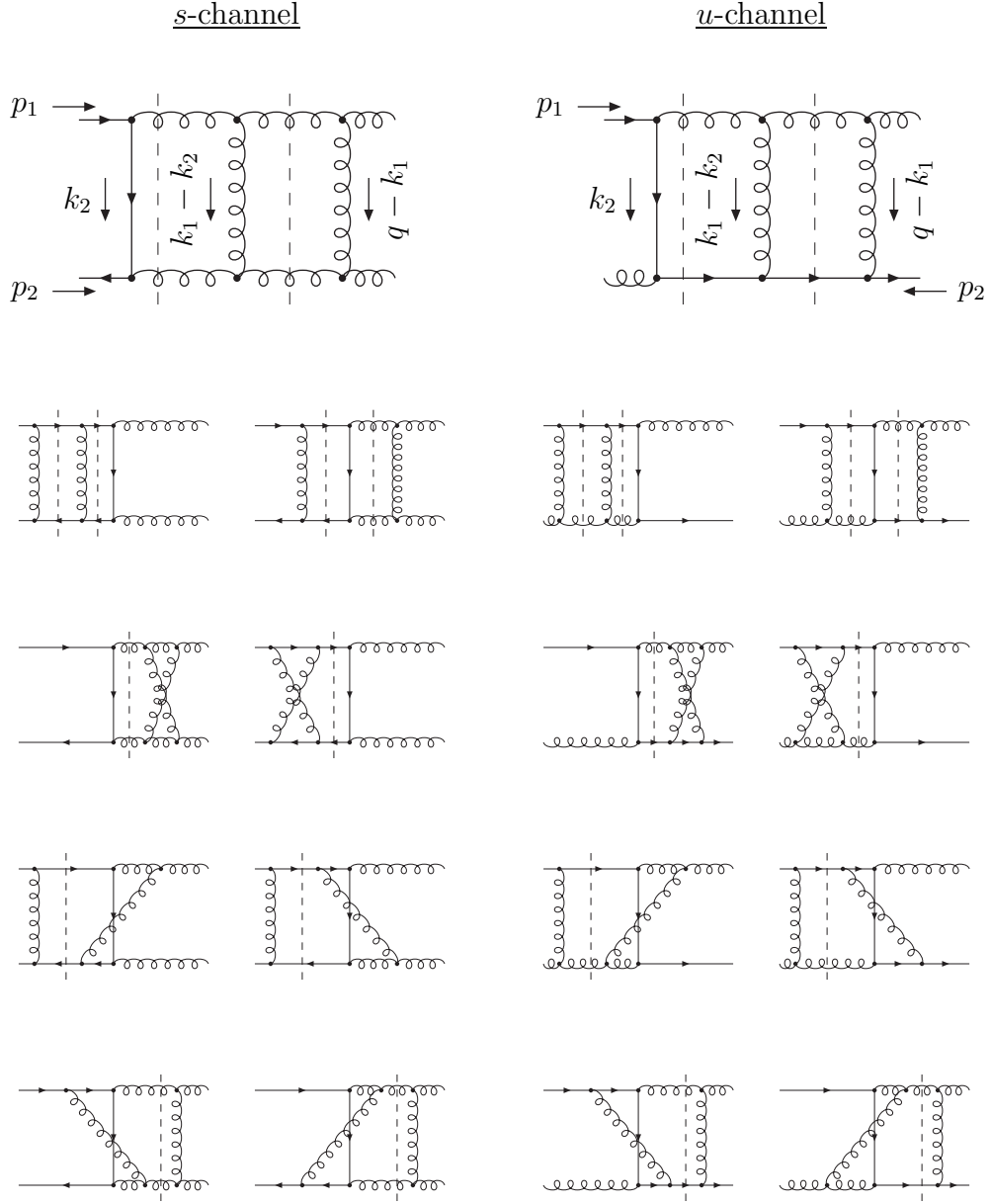


Figure 2.5: The complete set of leading  $\ln s$  two-loop, two particle cut diagrams



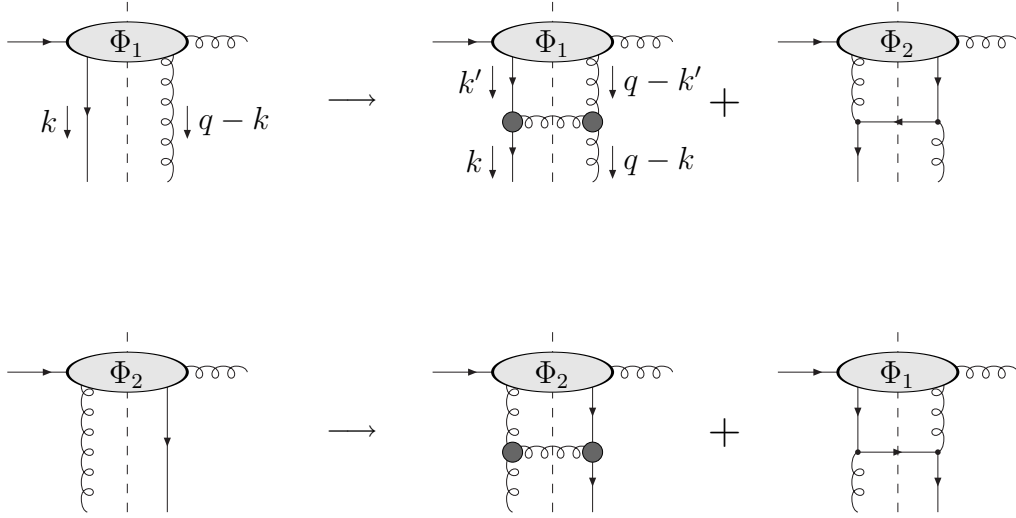


Figure 2.6: The addition of a rung involves the consideration of both a gluon rung with effective vertices and of a quark rung. Only the upper-half of the diagrams is shown, and note that the quark rung diagrams imply that we must have  $\Phi_1 = \Phi_2$

The first term is precisely what one would expect from the reggeization of the quark, whereas the second term cancels when we take into account the fact that the quark and gluon exchanged in the  $t$ -channel must themselves be reggeized and this reggeization gives rise to a correction

$$\int d^2\mathbf{k}' \mathcal{K}^{\text{regge}}(k, k', q) = (\epsilon_{\mathcal{Q}}(k) + \epsilon_{\mathcal{G}}(q - k)). \quad (2.14)$$

When all is pieced together we find that the effects of adding a rung *and* of taking into account the reggeization of the quarks and gluons exchanged in the  $t$ -channel is such that

$$\int d^2\mathbf{k}' (\mathcal{K}^{\text{rung}}(k, k', q) + \mathcal{K}^{\text{regge}}(k, k', q)) = \epsilon_{\mathcal{Q}}(q), \quad (2.15)$$

which means that the leading  $\ln s$  part of the amplitude, summed to all orders in perturbation theory, gives rise to an amplitude of the form

$$s^{\epsilon_{\mathcal{Q}}(q)} \mathcal{A}_0 \sim s^{1/2 + \epsilon_{\mathcal{Q}}(q)}, \quad (2.16)$$

where the “naïve”  $s$  dependence  $s^{1/2}$  arises from the usual  $s$  dependence of an amplitude in which a spin- $\frac{1}{2}$  particle is exchanged in the  $t$ -channel and is contained in the normalisation of the spinors in (2.2).

### 3 The Integral Equation for the Reggeon Amplitude and its Solution

The integral equation for the perturbative amplitude for processes involving the exchange of a Reggeon are obtained by considering ladders in which the vertical lines are a reggeized quark-antiquark pair, and the horizontal rungs are gluons which couple to these reggeized quarks via the effective vertex given in (2.7). The colour singlet is projected from the two fermions exchanged in the  $t$ -channel. This has been studied in [5]. One obtains an integral equation for the Mellin transform of the amplitude,  $f(s, k, q)$  defined by

$$\tilde{f}(\omega, k, q) = \int \frac{ds}{s} \left( \frac{s}{\mathbf{k}^2} \right)^{-\omega} f(s, k, q),$$

where  $k$  is the transverse momentum of the incoming quark and  $q$  is the momentum transfer (which may be taken to be transverse). In terms of this Mellin transform one obtains

$$\begin{aligned} \tilde{f}(\omega, k, q) = & \tilde{f}_0(\omega, k, q) + \frac{\tilde{\alpha}_s}{2\pi\omega} \int d^2\mathbf{k}' \left\{ \frac{\mathbf{k}' \cdot (\mathbf{k}' - \mathbf{q})}{\mathbf{k}'^2 (\mathbf{k}' - \mathbf{q})^2} \left[ \min \left( \frac{k}{k'}, \frac{k'}{k} \right) \right]^\omega \right. \\ & + \frac{\mathbf{k}' \cdot \mathbf{k}}{\mathbf{k}'^2 (\mathbf{k} - \mathbf{k}')^2} + \frac{(\mathbf{k} - \mathbf{q}) \cdot (\mathbf{k}' - \mathbf{q})}{(\mathbf{k}' - \mathbf{q})^2 (\mathbf{k} - \mathbf{k}')^2} \left. \right\} \tilde{f}(\omega, k', q) \\ & - \frac{\tilde{\alpha}_s}{2\pi\omega} \int d^2\mathbf{k}' \left\{ \frac{\mathbf{k}' \cdot \mathbf{k}}{\mathbf{k}'^2 (\mathbf{k} - \mathbf{k}')^2} + \frac{(\mathbf{k} - \mathbf{q}) \cdot (\mathbf{k}' - \mathbf{q})}{(\mathbf{k}' - \mathbf{q})^2 (\mathbf{k} - \mathbf{k}')^2} \right\} \tilde{f}(\omega, k, q), \quad (3.1) \end{aligned}$$

where we have used the notation

$$\tilde{\alpha}_s = C_F \frac{\alpha_s}{\pi},$$

and  $\tilde{f}_0(\omega, k, q)$  is the Born term obtained from the leading order contribution consisting of the exchange of a quark-antiquark pair (with no gluons).

There is an important difference between this equation and the equivalent equation [1] for the Pomeron, which is built out of reggeized gluons in a similar fashion. In the case of the Pomeron a solution which is of the reggeized form (i.e. a simple pole in the Mellin transform at a value of  $\omega$  equal to the Regge trajectory) is prevented by the fact that the colour factor which arises in the projection of a colour singlet from the two gluons in the  $t$ -channel is twice that obtained from the projection of a colour octet (relevant for the integral equation describing the reggeized gluon itself). In the case of the Reggeon, a colour factor of  $C_F$  is obtained *both* in the case of the reggeized gluon, and in the projection of a colour singlet from a quark-antiquark pair. In the Reggeon case, simple reggeization is prevented by the  $\omega$  dependent factor

$$\left[ \min \left( \frac{k}{k'}, \frac{k'}{k} \right) \right]^\omega,$$

which occurs inside the kernel on the RHS of (3.1). This term arises from the fact that when one exchanges fermions in the  $t$ -channel such that the momenta of these fermions appear in the numerators of the propagators, care must be taken in setting the kinematic limits of the phase-space integral over the longitudinal components of momentum [5]. It is these

kinematic limits which lead to the  $\omega$  dependent term in the kernel and, as we shall see later, this has a radical effect on the solution to this equation.

Henceforth we shall be confining our discussion to the case of zero momentum transfer ( $q = 0$ ), for which for which the second term on the RHS of (3.1) simplifies to

$$\begin{aligned} \tilde{\mathcal{K}}(\omega, k, k') \otimes \tilde{f}(\omega, k') = \frac{\tilde{\alpha}_s}{2} \int \frac{dk'^2}{k'^2} \left\{ \left[ \min \left( \frac{k}{k'}, \frac{k'}{k} \right)^\omega - 1 \right] \tilde{f}(\omega, k') \right. \\ \left. + \frac{k^2 + k'^2}{|k^2 - k'^2|} \left( \tilde{f}(\omega, k') - \tilde{f}(\omega, k) \right) + \tilde{f}(\omega, k) \right\}, \quad (3.2) \end{aligned}$$

where we have integrated over the angular part of  $k$ , assuming that the Reggeon is dominated by an amplitude which is azimuthally symmetric, i.e. that  $\tilde{f}(\omega, k')$  depends only on the magnitude,  $|k'|$ .

This can be solved exactly by exploiting the two-dimensional conformal invariance of the kernel to conclude that a function of the form

$$\tilde{f}(\omega, k) = (|k|^2)^{i\nu}$$

is an eigenfunction of the kernel with eigenvalue  $\omega(\nu)$  given by the solution to the equation

$$\omega = \frac{\tilde{\alpha}_s}{2} \left[ \frac{\omega}{\omega^2/4 + \nu^2} - 2\psi(1 + i\nu) - 2\psi(1 - i\nu) - 4\gamma_E \right]. \quad (3.3)$$

The leading eigenvalue is given by <sup>2</sup>

$$\omega_0 = \sqrt{2\tilde{\alpha}_s},$$

which implies that the Reggeon has an asymptotic  $s$  behaviour of the form

$$s^{\sqrt{2\tilde{\alpha}_s}}.$$

Another qualitative difference between the QCD Reggeon and the QCD Pomeron lies in the fact that such a leading  $s$  behaviour, which is not analytic in the coupling, cannot be reproduced in an ordinary perturbative expansion in  $\alpha_s$ , although the even orders in the expansion of this  $s$  dependence matches the double leading logarithms found in ordinary perturbation theory [6].

Thus, in principle, we have an analytic method for solving the integral equation for the Mellin transform of the Reggeon exchange amplitude. However, in order to be able to introduce further refinements, such as the running of the coupling or some simulation of non-perturbative effects which necessarily break the conformal invariance, one needs to be able to carry out a programme of numerical solution of (3.1).

---

<sup>2</sup> We note here that  $-\omega_0$  is also an eigenvalue of the kernel, and although it is sub-leading, it will turn out to be convenient to exploit this in our subsequent analysis.

This is most easily achieved by inverting the Mellin transform to obtain an integro-differential equation

$$\frac{\partial f(s, k)}{\partial \ln s} = \mathcal{K}(s, k, k') \otimes f(s, k'), \quad (3.4)$$

where

$$\begin{aligned} \mathcal{K}(s, k, k') \otimes f(s, k') = \tilde{\alpha}_s \left\{ \int_0^1 \frac{dz}{z} \frac{2z^2}{1-z^2} (f(s, kz) + f(s, k/z) - 2f(s, k)) \right. \\ \left. + \int_{1/s}^1 \frac{dz}{z} (f(sz, kz) + f(sz, k/z)) \right\} \end{aligned} \quad (3.5)$$

and we have introduced the variable  $z$  to represent  $\min(k/k', k'/k)$ . The  $\omega$  dependent part of the kernel in Mellin transform space is now encoded by the scaling of  $s$  by a factor of  $z$  in the appropriate terms.

We know that the asymptotic behaviour of the solution to this differential equation should be  $s^{\omega_0}$ . The usual method of numerical solution of such differential equations is to start with an initial function which has no  $s$  dependence and to integrate in steps using the Runge-Kutta method. Unfortunately, since the leading  $s$  behaviour arises from the  $\omega$  dependent part of the kernel in Mellin transform space, which has now been transferred to the  $s$  dependent part of  $f(s, k)$  on the RHS of (3.5), an initial function which does not contain any  $s$  dependence can *never* generate the expected asymptotic behaviour in any step-by-step numerical integration routine.

This difficulty can be circumvented by extracting the leading  $s^{\omega_0}$  behaviour. This is achieved by defining a function  $g(s, k)$  by

$$f(s, k) = \cosh(\omega_0 \ln(s)) g(s, k). \quad (3.6)$$

The asymptotic behaviour of  $f(s, k)$  is now displayed explicitly and we expect the function  $g(s, k)$  to have a far less dramatic  $s$  dependence. The integro-differential equation for  $g(s, k)$  is given by

$$\frac{\partial g(s, k)}{\partial \ln s} = \operatorname{sech}(\omega_0 \ln s) \mathcal{K}(s, k, k') \otimes (\cosh(\omega_0 \ln s) g(s, k')) - \omega_0 \tanh(\omega_0 \ln s) g(s, k) \quad (3.7)$$

where the kernel  $\mathcal{K}(s, k, k')$  is defined in (3.5). We note here that  $g(s, k) = \text{constant}$  is an exact solution of (3.7). We may therefore start with a function,  $g_0(k)$ , that depends only on  $k$  but *not* on  $s$  (which one would normally obtain from an “impact factor” which encodes the coupling of the Reggeon to the particles between which the Reggeon is exchanged) and generate (after sufficient iterations) a solution for the Reggeon exchange amplitude with initial value  $g_0(k)$  taken as the value of the amplitude at low  $s$ .

We have checked numerically that this method reproduces the known analytic results in the case of a trial initial function, which has a simple Fourier transform. We have taken

$$g_0(k) = \frac{|k|^2}{(|k|^2 + 1)^2} = \frac{1}{\pi} \int_0^\infty d\nu \Gamma(1 + i\nu) \Gamma(1 - i\nu) (|k|^2)^{i\nu}. \quad (3.8)$$

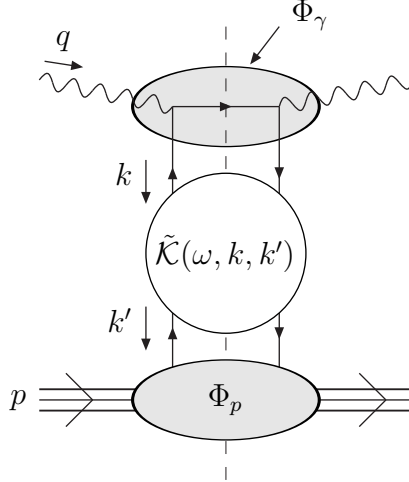


Figure 4.1: The impact factors  $\Phi_\gamma$  and  $\Phi_p$  encode how the virtual photon (or  $W$ -,  $Z$ -boson) and the proton respectively couple to the Reggeized quark ladder. The central circle symbolises the kernel’s role in adding rungs and Reggeizing the uprights

For large  $s$  the amplitude is then given by

$$f(s, k) = \frac{1}{\pi} \int_0^\infty d\nu \Gamma(1 + i\nu) \Gamma(1 - i\nu) (|k|^2)^{i\nu} s^{\omega(\nu)}, \quad (3.9)$$

where  $\omega(\nu)$  is given by (3.3). This can be compared with the numerical method described above. Having established the validity of this numerical approach, one can introduce refinements to the kernel, which render it intractable to analytical methods, but still open to numerical analysis. In the next section we discuss the results of such an approach.

## 4 Numerical Results

In this section we apply the technique discussed in the last section to a model of deep-inelastic scattering processes at low- $x$ , which would be dominated by Reggeon rather than Pomeron exchange (such as the structure function  $F_3$  for virtual  $W$ - or  $Z$ -boson scattering, or the spin-dependent structure functions which are intrinsically flavour non-singlet). For the rest of this section we shall use the term “structure function” to mean the flavour non-singlet part of a structure function, which we expect to be dominated by Reggeon exchange at low- $x$ . In order to do this we need some model for the “impact factors” which account for the coupling of the Reggeon at the top and bottom of the ladder, as indicated in Fig. 4.1. Unlike the case of the Pomeron, there is a direct coupling of the quarks in the Reggeon to the virtual particle involved in the scattering (photon,  $W$ -boson, or  $Z$ -boson). This means that the upper impact factor is proportional to

$$\delta(k^2 - Q^2),$$

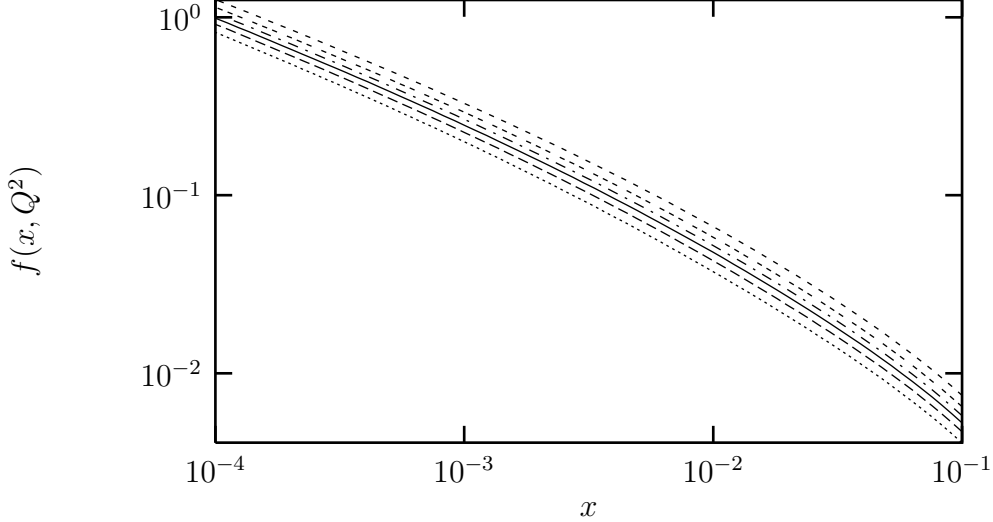


Figure 4.2: The (lack of) dependence of results on the parameter  $\eta$  in (4.1) is demonstrated. The structure function at fixed  $Q^2$  is given for six values of  $\eta$  from 0.6 to 2.0

where  $-Q^2$  is the square momentum of the virtual boson. At the other end of the ladder we need the impact factor for the coupling of the Reggeon to the target proton. This is non-perturbative in nature and so we model this with the simple form

$$\Phi_p \propto e^{-k^2/\eta\Lambda_{\text{QCD}}^2}, \quad (4.1)$$

where we expect  $\eta$  to be of order unity, and we have not fixed the constant of proportionality which means that our scale remains arbitrary. This is clearly a crude estimate of the lower impact factor, but we do not expect our results for the low- $x$ , large  $Q^2$  regime to depend critically on the exact form of this impact factor. This is because after a sufficient number of iterations of the kernel one expects the amplitude to lose all “memory” of the initial condition. As a demonstration of this, we show in Fig. 4.2 the variation of the structure function plotted against  $x$  for  $Q^2 \sim 100 \text{ GeV}^2$  for a range of the parameter  $\eta$  between 0.6 and 2.0. We see that the variation of the shape of the structure is indeed small and the differences can be substantially absorbed into an overall normalization.

We start by assuming fixed coupling. In this case the behaviour of the structure function at low  $x$  for each value of  $Q^2$  was obtained by starting with an initial function given by (4.1) and numerically integrating (3.7) using the Runge-Kutta method with the coupling  $\tilde{\alpha}_s$  taken to be  $\tilde{\alpha}_s(Q^2)$ . From the resulting function  $f(x, k)$  ( $s$  is replaced by  $1/x$ ), the point  $k^2 = Q^2$  was selected, thereby imposing the delta-function which represents the impact factor at the top of the ladder. This process was then repeated for different values of  $Q^2$ .

Next we wish to include the effect of the running of the coupling. This is achieved by promoting the coupling  $\tilde{\alpha}_s$  in the expression for the kernel to a running coupling. We take the larger of the momenta  $k$  and  $k'$  as the argument of the running of the coupling, which means that the coupling must now be taken *inside* the integral in (3.5). One immediate

effect of this is that the quantity  $\omega_0$ , which was the leading eigenvalue of the kernel in the case of fixed coupling, now becomes a function of  $k$  given by

$$\omega_0(k) = \frac{1}{2} \int \frac{dk'^2}{k'^2} \tilde{\alpha}_s(\max(k, k')) \left[ \min\left(\frac{k}{k'}, \frac{k'}{k}\right) \right]^{\omega_0(k^2)}, \quad (4.2)$$

and it is this value of  $\omega(k)$  that is used to factor off the leading behaviour. Thus we define  $g(x, k)$  as

$$f(x, k) = \cosh(\omega(k) \ln(s)) g(x, k),$$

and the  $x$  dependence of  $g(x, k)$  is given by (3.7) with  $\tilde{\alpha}_s$  replaced by  $\tilde{\alpha}_s(\max(k, k'))$ . Note that in this case, unlike the case of fixed coupling, we only need to solve the corresponding differential equation once, since the argument of the coupling for each iteration does *not* now depend on  $Q^2$ . A single pass through the range of  $x$  returns a function  $f(x, k)$  and the results for the structure function at any value of  $Q^2$  can be read off by setting  $k^2 = Q^2$ .

As is always the case when we introduce a running coupling in such integro-differential equations, we need to impose an infra-red cutoff below which  $\alpha_s$  takes the value  $\alpha_{\max}$  and ceases to run. This is because the integral in (3.5) samples *all* possible momenta so that without the imposition of such an infra-red cutoff one would run into the Landau pole. We have chosen  $\alpha_{\max}$  to take the value 1.

In Figs. 4.3 and 4.4, we show the resulting structure function  $f(x, Q^2)$  plotted against  $x$  for different values of  $Q^2$ . Fig. 4.3 refers to fixed coupling and Fig. 4.4 to running coupling. We have also displayed a curve indicating the  $x^{-1/2}$  dependence that one would expect to obtain from the naïve counting of amplitudes in which spin- $\frac{1}{2}$  particles are exchanged in the  $t$ -channel. The enhancement at low- $x$  is clearly seen and at sufficiently low- $x$  the structure function behaves like

$$f(x, Q^2) \sim x^{-1/2 + \sqrt{2\tilde{\alpha}_s(Q^2)}},$$

for the case of fixed coupling, and for running coupling we have an even further enhancement of the low- $x$  rise which asymptotically behaves like

$$f(x, Q^2) \sim x^{-1/2 + \sqrt{2\alpha_{\max}}}.$$

On the other hand, we see from Figs. 4.5 and 4.6 that there is much less  $Q^2$  dependence in the rise at low- $x$  when the running of the coupling is taken into account. This is consistent with recent results [7] obtained in the case of the Pomeron with running coupling. This can be attributed to the fact that for the  $Q^2$  dependence of the structure functions at low- $x$ , the effect of running the coupling is to sample values of  $k^2$  which are larger than  $Q^2$  for which the running coupling is smaller than the fixed coupling value, whereas for the  $Q^2$  independent part one is also probing the infrared region where the running coupling is enhanced.

Finally, we consider possible non-perturbative effects. One important consequence of non-perturbative QCD is that quarks acquire a constituent mass. As soft quarks are exchanged in the  $t$ -channel in the Reggeon, it is quite likely that this will be the most significant contribution of non-perturbative QCD to the behaviour of the Reggeon. We also choose to give the soft gluons an effective mass, and so to simulate the effects of non-perturbative QCD we assigning a mass,  $m$ , to the soft quarks and gluons.

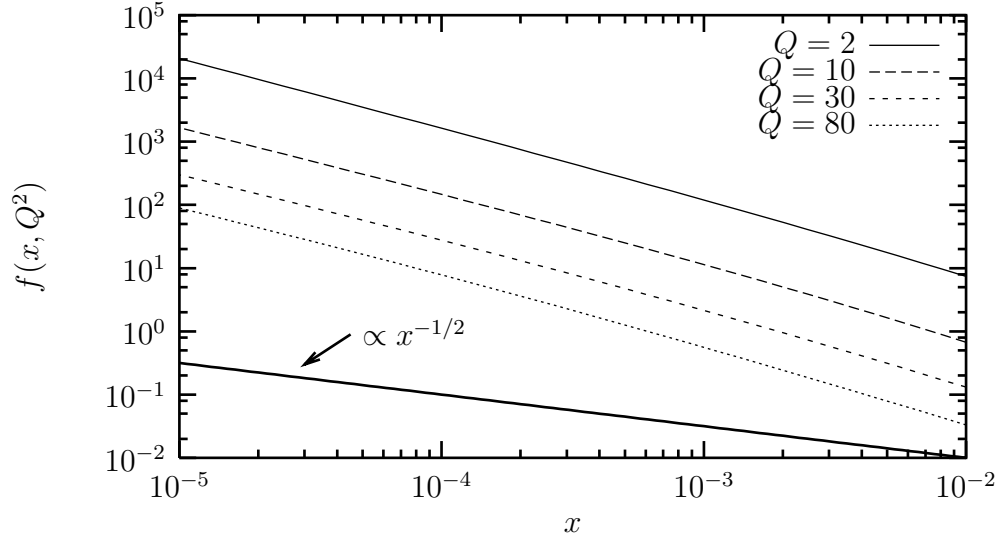


Figure 4.3: The rise in the structure function at low- $x$  is shown here for four different values of  $Q$  (in [GeV]) for static  $\alpha_s$ . The naïve dependence of  $x^{-1/2}$  is also shown for comparison

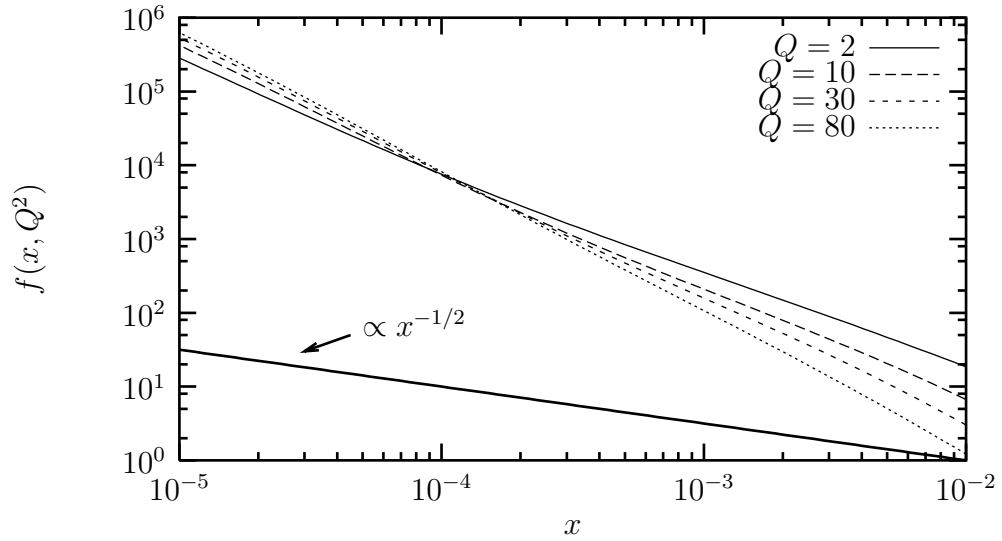


Figure 4.4: The same as figure 4.3 but with a running coupling. Note that the low- $x$  rise is now even more pronounced



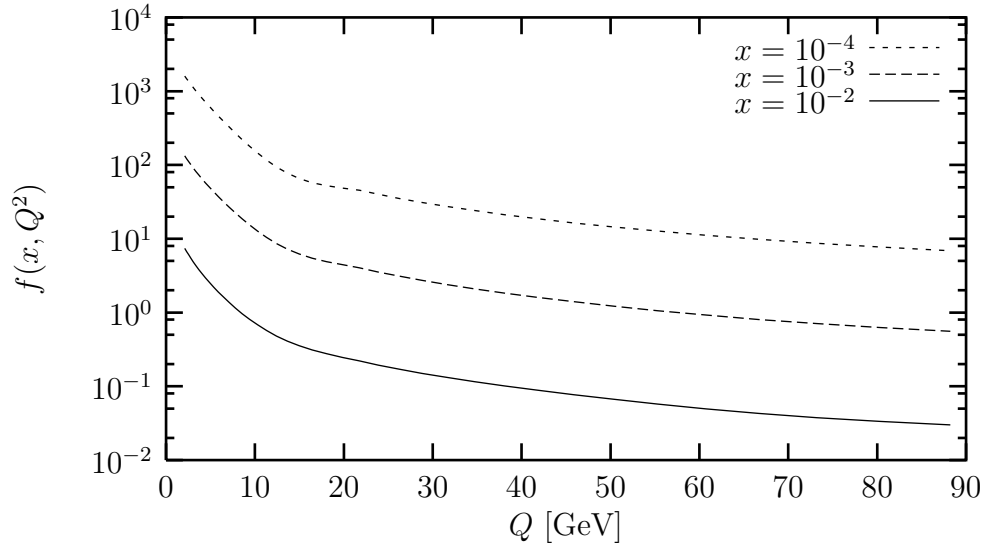


Figure 4.5: The structure function  $f$  shown against  $Q$  for three values of  $x$ . The coupling has been fixed for this calculation

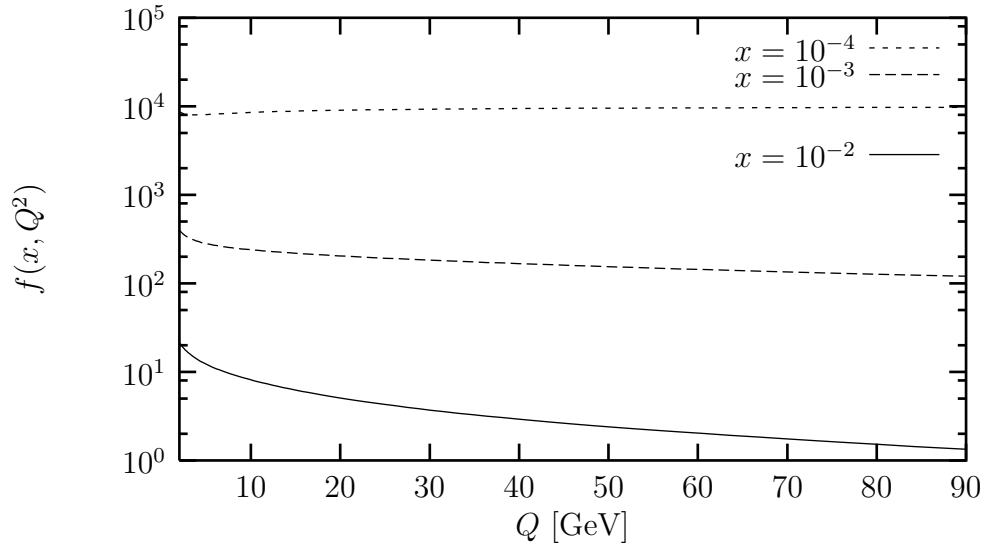


Figure 4.6: Similar to figure 4.5, but with the coupling now running. This acts to reduce the rise at small  $Q$

The kernel (3.5) then becomes

$$\begin{aligned}
\mathcal{K}_m(s, k, k') \otimes f(s, k') = & \int_0^1 \frac{dz}{z} \left[ \tilde{\alpha}_s(k^2) \frac{z^2}{z^2 + M^2} \left( \frac{1 + z^2 + M^2}{\sqrt{((1+z)^2 + M^2)((1-z)^2 + M^2)}} - 1 \right) \right. \\
& \times (f(s, kz) - f(s, k)) + \tilde{\alpha}_s(k^2/z^2) \frac{1/z^2}{1/z^2 + M^2} \\
& \times \left. \left( \frac{1 + 1/z^2 + M^2}{\sqrt{((1+1/z)^2 + M^2)((1-1/z)^2 + M^2)}} - 1 \right) (f(s, k/z) - f(s, k)) \right] \\
& + \int_{1/s}^1 \frac{dz}{z} \left[ \tilde{\alpha}_s(k^2) \frac{z^2}{z^2 + M^2} f(sz, kz) + \tilde{\alpha}_s(k^2/z^2) \frac{1/z^2}{1/z^2 + M^2} f(sz, k/z) \right], \quad (4.3)
\end{aligned}$$

in which we have defined  $M^2 = m^2/k^2$ .

The expression for  $\omega_0(k)$  then becomes

$$\omega_0(k^2) = \frac{1}{2} \int \frac{dk'^2}{k'^2 + m^2} \tilde{\alpha}_s(\max(k^2, k'^2)) \left[ \min\left(\frac{k}{k'}, \frac{k'}{k}\right) \right]^{\omega_0(k^2)}. \quad (4.4)$$

and it is this expression for  $\omega_0(k^2)$  which is used to define  $g(s, k)$  in (3.6).

The introduction of the mass term acts to reduce the value of  $\omega_0$ , and a plot of this effect is given in Fig. 4.7. Note that the smaller  $Q^2$  values receive a more marked decrease in the leading eigenvalue, which further acts to limit growth in the infra-red region.

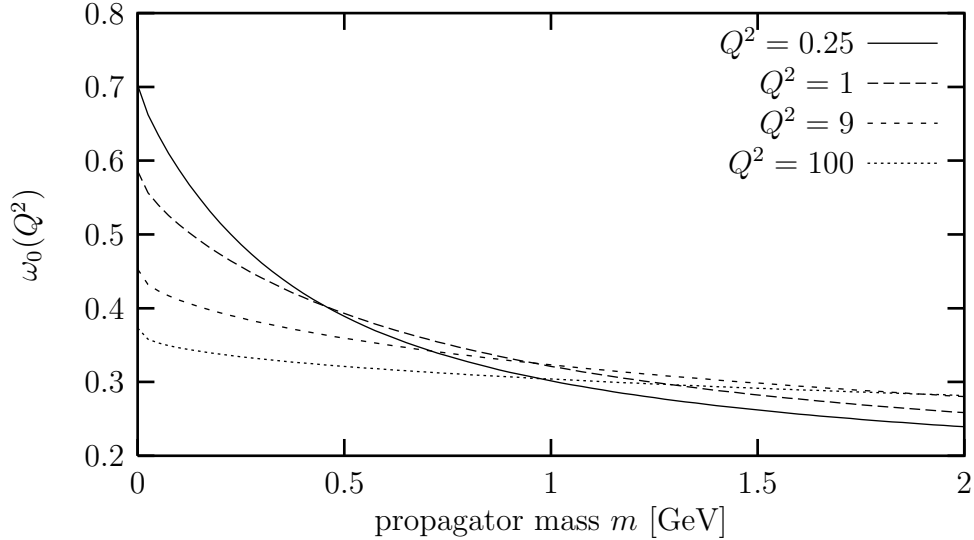


Figure 4.7: The variation of the leading eigenvalue with propagator mass, shown for four different values of  $Q^2$  (all given in  $\text{GeV}^2$ )

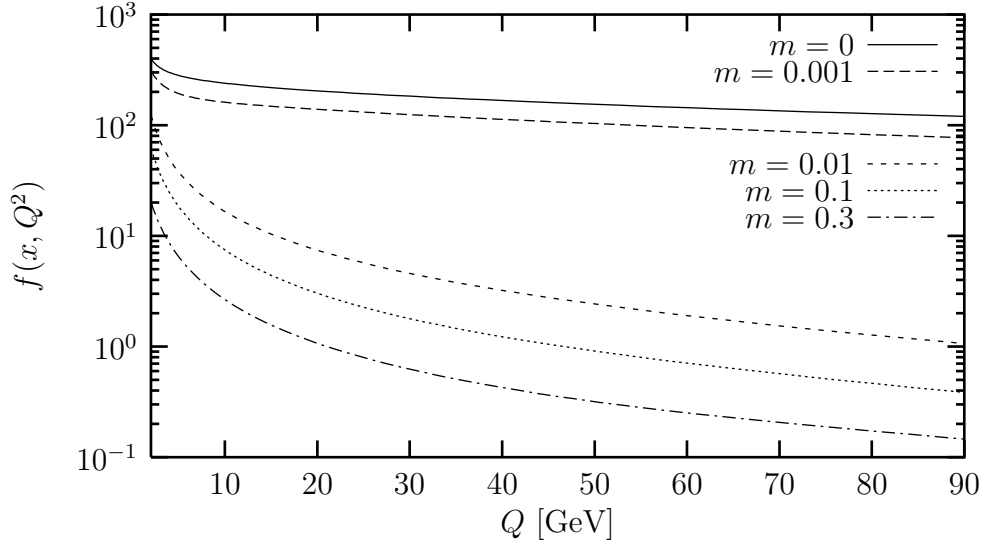


Figure 4.8: The effect of non-zero propagator masses is shown at  $x = 10^{-3}$ . Increasing the mass (all in GeV) leads to a reduction at large  $Q$  due to the decrease in the leading eigenvalue  $\omega_0$

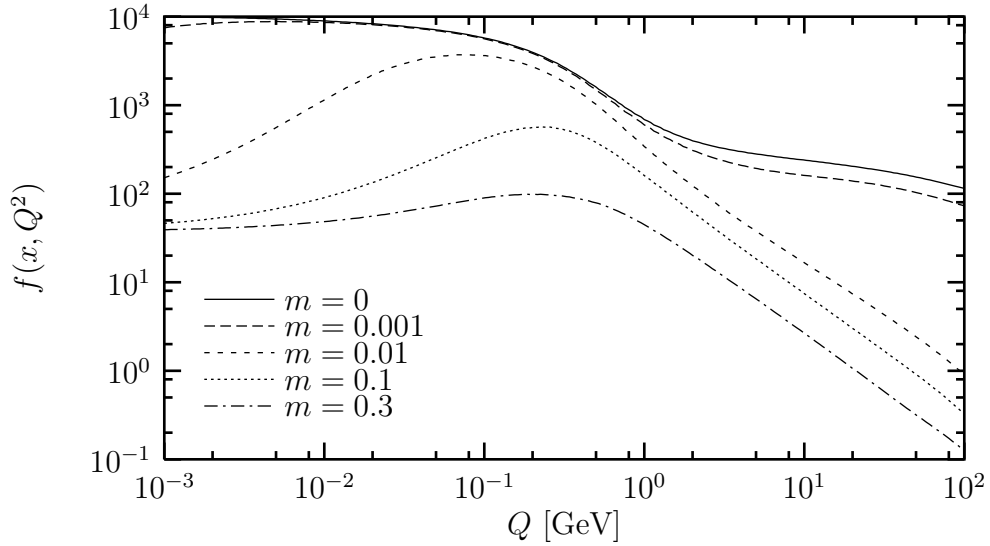


Figure 4.9: The same data as in figure 4.8 is shown here with a logarithmic x-axis to demonstrate the infra-red effects of the propagator mass

We show the effect of the massive propagators in Fig. 4.8. Here we have plotted against  $Q$  for five values of  $m$ , including  $m = 0$ . The effect is quite strong, even at larger values of  $Q$ , with the reduction in  $f$  being more pronounced than might be expected of a measure originally designed to affect just the infra-red region. The reason behind this has of course just been detailed: increasing  $m$  reduces  $\omega_0$  so that by the time we have evolved the structure function to low- $x$  (the graph is at  $x = 10^{-3}$ ) it is substantially reduced across its whole domain due to the weaker leading behaviour. If we were to consider the same function at larger  $x$  the differences between the graphs for differing  $m$  would not be so pronounced for large  $Q^2$ .

In Fig. 4.9 we have shown exactly the same data as in the previous graph, but with the  $Q$  scale now logarithmic in order to illustrate the small  $Q$  region more clearly. As expected, the introduction of the mass term results in a reduction at low  $Q$ , but whereas the larger  $Q$  reduction only becomes apparent as we evolve to low- $x$ , the growth in the  $Q \sim m$  region is immediately regulated.

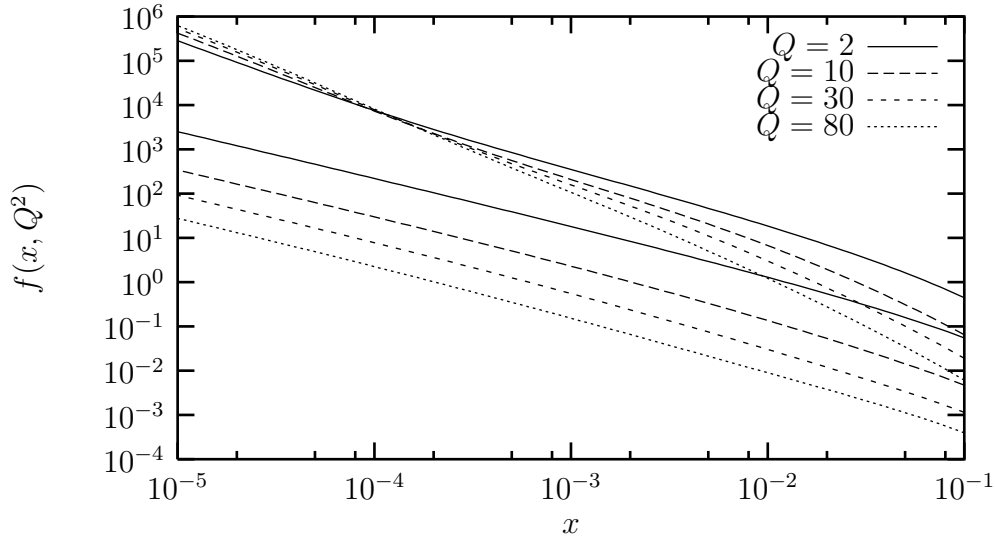


Figure 4.10: The upper set of four lines show zero mass results to provide comparison with the lower set which have  $m = 0.3$  GeV. As expected the rise at low  $x$  has been slowed by the non-zero mass

In Fig. 4.10 we have again plotted the zero mass/running coupling graphs for four  $Q$  values, but we have also included on the same plot the case where we take  $m = 0.3$  GeV. Thus the upper set of lines are the same as in figure 4.4, and the lower set show the relative effect of the propagator's mass. As would be expected from our previous arguments the low- $x$  rise in  $f$  is reduced.

## 5 Summary

We have reviewed the derivation of the reggeization of the quark. This reggeized quark is used to construct the integro-differential equation for the amplitude of a process in which the quantum numbers of the Reggeon are exchanged. We have proposed a method for the numerical solution of this equation which is consistent with the leading large  $s$  behaviour. This enables one to make modifications to the kernel in order to account for a running coupling and for simulations of non-perturbative effects.

The experimental quantities which can be used for probing the QCD simulated Reggeon are flavour non-singlet quantities at low- $x$ . In all probability the reach of current experiments in deep-inelastic scattering are not yet sufficient provide us with such a probe, but it may well become possible in the near future.

We find from our numerical studies that the introduction of the running of the coupling enhances the already sharp rise expected in the structure functions as  $x \rightarrow 0$ . On the other hand the  $Q^2$  dependence is considerably moderated when a running coupling is introduced. The effects of QCD beyond perturbation theory have been estimated by assigning a mass to the soft particles exchanged. We find that this has a dramatic effect in reducing the rise at low- $x$ , even at values of  $Q^2$  which are considerably larger than the values of the constituent mass inserted. All of this suggests that it will be even harder to isolate the kinematic region where we might expect the results of perturbative QCD to dominate, and although a rise at low- $x$  is still expected, it may well not be as dramatic as initially expected.

## References

- [1] E. A. Kuraev, L. N. Lipatov and V. S. Fadin, *Sov. Phys. JETP* **44**:443 (1976); *ibid.* **45**:199 (1977); Y. Y. Balitski and L. N. Lipatov, *Sov. J. Nucl. Phys.* **28**:822 (1978)
- [2] A. Donnachie and P. V. Landshoff, *Nucl. Phys.* **B244**:332 (1984); *Phys. Lett.* **B296**:227 (1992)
- [3] B. Badalek and J. Kwiecinski, *Phys. Lett.* **B418**:229 (1998)
- [4] V. S. Fadin and V. E. Sherman, *Sov. Phys. JETP* **45**:801 (1977)
- [5] R. Kirschner, *Z. Phys.* **C31**:135 (1986); *ibid.* **C65**:505 (1995); **C67**:459 (1995)
- [6] R. Kirschner and L. N. Lipatov, *Nucl. Phys.* **B213**:122 (1983)
- [7] R. S. Thorne, (1999) hep-ph/9803445